

# Measurements of neutron capture effects on Cd, Sm and Gd in lunar samples with implications for the neutron energy spectrum

D.G. Sands<sup>1</sup>, J.R. De Laeter, K.J.R. Rosman<sup>\*</sup>

*Department of Applied Physics, Curtin University of Technology, G.P.O. Box U1987, Perth, W.A. 6485, Australia*

Received 13 March 2000; accepted 3 January 2001

## Abstract

The bombardment of the lunar surface by cosmic rays produces secondary neutrons, some of which are thermalized by the lunar soil and then interact strongly with the isotopes of Cd, Gd and Sm which have high neutron capture cross sections at thermal energies causing changes in their isotopic compositions. We have measured these changes in samples from the Apollo 14, 16 and 17 missions using thermal ionization mass spectrometry. Changes of  $^{114}\text{Cd}/^{113}\text{Cd}$  of 0.3–0.5% in samples 60501,105, 65701,23 and 72161,73, of 0.4 and 0.8% in  $^{158}\text{Gd}/^{157}\text{Gd}$  in samples 14163,848 and 60501,105 and of 0.8, 1.2 and 0.06% for  $^{150}\text{Sm}/^{149}\text{Sm}$  in samples 14163,848 and 60501,105 and 74220,125 respectively, have been observed. This is the first time that neutron capture on Cd has been detected in lunar samples. Thermal neutrons are captured preferentially at resonance energies of 0.03 eV by  $^{155}\text{Gd}$  and  $^{157}\text{Gd}$ , at 0.09 eV by  $^{149}\text{Sm}$  and at 0.178 eV by  $^{113}\text{Cd}$ . A comparison of the changes in  $^{114}\text{Cd}/^{113}\text{Cd}$ ,  $^{156}\text{Gd}/^{155}\text{Gd}$ ,  $^{158}\text{Gd}/^{157}\text{Gd}$  and  $^{150}\text{Sm}/^{149}\text{Sm}$  due to neutron capture can therefore indicate the energy distribution of the neutrons. Previous work has compared changes in  $^{158}\text{Gd}/^{157}\text{Gd}$  and  $^{150}\text{Sm}/^{149}\text{Sm}$ , while this study extends the comparison to  $^{114}\text{Cd}/^{113}\text{Cd}$ , where the resonance energy is significantly higher. This has enabled us to confirm evidence for a harder neutron energy spectrum in lunar soil than is predicted theoretically. This can be seen in significantly higher capture rates than predicted for  $^{149}\text{Sm}$  compared to  $^{157}\text{Gd}$ . We also present evidence of enhanced capture rates on  $^{113}\text{Cd}$  compared with  $^{149}\text{Sm}$  and  $^{157}\text{Gd}$ . The concentrations of Cd, Gd and Sm in nine lunar samples have also been measured by isotope dilution mass spectrometry with Cd being measured in lunar samples for the first time by this method. While Cd was found to be heterogeneously distributed in some samples, Gd and Sm showed good agreement with previous measurements, except for sample 14163,848 where it was significantly lower. © 2001 Elsevier Science B.V. All rights reserved.

**Keywords:** neutron capture; mass spectroscopy; isotope dilution; energy spectrum; moon; cadmium; gadolinium; samarium

## 1. Introduction

Cosmic ray bombardment of the lunar surface produces a variety of secondary particles including neutrons that are thermalized in the lunar soil. These neutrons are preferentially captured by isotopes with high capture cross sections such as

<sup>\*</sup> Corresponding author. Fax: +61-8-9266-2377;  
E-mail: rrosmank@cc.curtin.edu.au

<sup>1</sup> Present address: Land Operations Division, P.O. Box 1500, Salisbury 5108, Australia.

$^{113}\text{Cd}$ ,  $^{149}\text{Sm}$ ,  $^{155}\text{Gd}$  and  $^{157}\text{Gd}$  ( $2.06 \times 10^4$ ,  $4.01 \times 10^4$ ,  $6.09 \times 10^4$  and  $2.540 \times 10^5$  barns at resonance respectively: N. Holden, Brookhaven National Lab., USA, personal communication). These reactions have been measured for Sm and Gd in meteorites [1,2,11] and in lunar samples [3–10,12] but although evidence of neutron capture on Cd has been sought in meteorites [13] it has not been detected. No previous measurements have been made on Cd isotopes in lunar material.

Isotopes  $^{113}\text{Cd}$ ,  $^{149}\text{Sm}$  and  $^{155}$  and  $^{157}\text{Gd}$  have resonance energies for neutron capture at 0.178, 0.0973, 0.0268, and 0.0314 eV respectively. However, the energy spectrum of the thermal neutrons in the lunar surface is still not well known. Three decades ago Lingenfelter et al. [14] constructed a theoretical energy spectrum for neutrons in lunar soil in order to calculate relative changes in the isotopic composition of these and other isotopes. Although this work has provided a valuable basis for experimental studies, measurements of relative changes in the abundance of Gd and Sm isotopes suggest that the neutron energy spectrum in lunar soil is harder than expected from theoretical considerations [12].

Here we extend the earlier isotopic work on lunar samples to include measurements of neutron capture on  $^{113}\text{Cd}$  and in so doing explore a significantly higher energy region of the neutron spectrum. The work also provides concentration measurements of Cd in lunar rock and soils by isotope dilution mass spectrometry (IDMS), an accurate method that has not been used previously. Because earlier studies did not include some samples analyzed here, complementary measurements were also made of Gd and Sm isotopes in these samples.

## 2. Experimental procedures

### 2.1. Samples

Lunar samples were stored inside a clean-air laboratory in the aluminum capsules received from the NASA lunar sample curators. After weighing each sample, the material was immediately re-sealed.

Nine lunar soil samples were analyzed in this study, 10017,341 (vesicular basalt, high Ti mare basalt), 14163,848 (surface soil sample), 14310,615 (polymict rock melted on impact), 15041,188 (near surface soil sample), 15059,240 (interior chips from a regolith breccia containing mixed fragments), 60501,105 (surface soil), 65701,23 (surface soil), 72161,73 (surface soil) and 74220,125 (orange glass). Five of the samples have been previously measured for Sm and Gd isotopic abundances.

### 2.2. Sample processing

Dissolution and separation of the samples followed the general procedures described in [15]. Samples were digested by the progressive application of HF,  $\text{HNO}_3$  and HCl. For concentration measurements tracers enriched in  $^{106}$  and  $^{111}\text{Cd}$ ,  $^{152}\text{Gd}$ , and  $^{147}\text{Sm}$  were added to 5% of the sample, at the end of the digestion procedure.

Separation and purification of the Cd and rare earths followed the ion exchange procedures described in [15]. Two anion columns and one cation column were used to separate the Cd. The rare earth elements (REE) and the other matrix elements were eluted from the first anion exchange column in concentrated HCl. Silver, Sn and In were removed by the application in turn of HCl, a HF/HCl mixture and HCl, while the Cd was eluted in  $\text{HNO}_3$ . The inclusion of a second anion column improved the purity of the separated Cd. In the final cation exchange column the Cd was eluted with HCl.

The REE washed from the first anion column were separated from the matrix elements on a cation column using a modification of the procedures described by [16]. Gd and Sm were separated by HPLC [17] and in a final stage using Eichrom Lanthanide resin. The digestion procedure left a small residue of negligible weight in samples 10017, 15041, 60501, 65701 and 74220. The overall extraction efficiency was about 96, 70 and 78% for Cd, Gd and Sm respectively, as determined by IDMS.

### 2.3. IDMS

All samples were measured by thermal ionization mass spectrometry (TIMS) and concentrations were determined using the IDMS method [18]. For IDMS analyses materials enriched in  $^{106}\text{Cd}$ – $^{111}\text{Cd}$  (enriched to 24.6 and 66.5%, respectively),  $^{152}\text{Gd}$  (enriched to 41.2%), and  $^{147}\text{Sm}$  (enriched to 98.3%) (Oak Ridge National Laboratory, USA) were used. Solutions of these isotopes were calibrated against gravimetrically prepared solutions using IDMS. For the Cd concentrations the isotope pairs 111/112 and 111/113 were used for the IDMS calculations, for Gd 152/160 and 152/158 and for Sm 147/152 and 147/149.

### 2.4. Mass spectrometry

Isotopic analysis followed the procedures described in [15]. Samples, loaded onto Re filaments, were analyzed in a VG 354 TIMS fitted with a 16-sample turret, nine Faraday cup collectors and a Daly detector.

Cd was loaded in silica gel and phosphoric acid onto a single Re filament. The samples, which were typically less than 50 ng, were measured on the Faraday multi-cup collector system giving uncertainties for  $^{114}\text{Cd}/^{112}\text{Cd}$  of  $\sim 0.03\%$  at the 95% confidence level for Cd ion currents of  $\sim 1 \times 10^{-12}$  A.

Gadolinium was loaded onto the side filaments of a triple Re filament assembly in an aqueous solution of methyl lactic acid and the metal ions were measured. Measurements yielded uncertainties at the 95% confidence level of 0.05% for  $^{158}\text{Gd}/^{160}\text{Gd}$  on the multi-collector Faraday cup system with ion currents of  $\sim 1 \times 10^{-12}$  A.

Samarium samples were loaded in HCl on the side filaments of a triple Re filament assembly, yielding total ion currents  $\sim 1 \times 10^{-11}$  A and typical uncertainties at the 95% confidence level for  $^{152}\text{Sm}/^{154}\text{Sm}$  of 0.005%.

### 2.5. Interferences

#### 2.5.1. Cadmium

Isobaric interference from Pd (isotopes 106, 108 and 110), Sn (isotopes 112, 114 and 116) and In

(isotope 113) are possible. During measurements visual checks were always made but no Pd interference was detected. Interference from In and Sn isotopes were also visually monitored at masses 115 and 118 respectively, although none was detected. However, in some of the smaller samples isotopic ratio measurements indicated that the  $^{116}\text{Cd}$ , was enhanced, consistent with interference from Sn.

An iterative procedure, described in [19], was used to correct Cd isotopes 112, 114 and 116 for Sn interference. This was achieved by progressively decreasing the tin contribution to the three affected isotopes until the 113 depletion and 114 excess conformed to the theoretical proportions for neutron capture. In making this adjustment it is unavoidable that some bias, within the uncertainties, may occur in the  $^{113}\text{Cd}/^{114}\text{Cd}$  ratio. The contribution at isotope 116, where Sn is the most abundant (atom abundance of  $^{116}\text{Sn}$  is 14.4%), was  $\leq 1.2\%$  of the  $^{116}\text{Cd}/^{112}\text{Cd}$  ratio in the worst case. The effects at 112 and 114 were much smaller, since the  $^{112}\text{Sn}$  and  $^{114}\text{Sn}$  abundances are 1 and 0.65% respectively.

Interference from  $\text{CaPO}_2$  and related molecular ions occurred at low temperatures at mass positions 106, 108 and 110 in early analyses, but this interference was reduced to negligible levels in later analyses by more efficient separation of Ca from the Cd sample during chemical processing and by more extensive degassing of the sample in the mass spectrometer.

#### 2.5.2. Gadolinium

Sm, SmO, BaF, BaO, Dy and several rare earth oxides can interfere with Gd metal ions. Efficient chemistry removed most of the rare earths from the sample, but contributions from LaO were checked at mass 155, from NdO at masses 158 and 160, from Dy at 156, 158 and 160 and from Sm at 152 and 154. However, La, Nd and Dy evaporate at lower temperatures than Gd, so do not usually cause a problem. As Sm isotopes are not isobaric with  $^{155-160}\text{Gd}$  where neutron capture occurs, any interference from Sm would not affect these ratios. BaO was rarely detected, and was not present at the higher temperatures needed to ionize Gd. Interference from BaF, which can inter-

ferre at  $^{154}\text{Gd}$  to  $^{157}\text{Gd}$ , was negligible at the high temperatures used to ionize Gd. It could be monitored at 149, 151 or 153, though at 149 it could be concealed by Sm and at 151 and 153 by Eu.

### 2.5.3. Samarium

Only Gd, Nd or BaF are likely to interfere with Sm metal ions. Nd was rarely present and in any event, evaporates at a low temperature, whereas Gd requires too high a temperature for ionization to interfere with Sm. BaF interference was monitored at mass 157 and no correction was necessary.

## 3. Results and discussion

Cd, Gd and Sm concentrations in lunar samples measured by IDMS are listed in Table 1.

### 3.1. Concentration measurements

#### 3.1.1. Cadmium

These are the first measurements of Cd in lunar material to be made by IDMS. All measurements

were corrected for analytical blanks, measured with each set of samples; these were in the range 90–170 pg. Most lunar samples had concentrations between 1.5 and 300 ng/g, but some were much higher. These values were not always in agreement with earlier measurements by neutron activation analysis. The largest discrepancy occurred for sample 10017 where the IDMS value was a factor of  $\sim 7$  times lower and for sample 60501 where one IDMS measurement was two orders of magnitude higher than a replicate measurement which was in reasonable agreement with a literature value. Because of the limited quantity of sample available few replicate analyses were made. For a homogeneous sample the concentrations should agree to within the uncertainties shown [15]. In the case of sample 60501 the sample with the higher concentration showed the greater depletion in  $^{113}\text{Cd}$  discounting the possibility that it was contaminated with terrestrial Cd. A cause of some of the differences between this work and published values is therefore sample heterogeneity. In an effort to minimize contamination of the samples no attempt was made to grind or homogenize them. On the other hand

Table 1  
Cadmium, gadolinium and samarium concentrations<sup>a</sup> in lunar samples

Sample	Concentration <sup>b</sup> This work	Literature values for similar samples
<i>Cadmium (ng/g)</i>		
10017,341	10.0 ± 0.2	68 [27] #10017,87
14163,848	1.04 ± 0.02 μg/g, 0.80 ± 0.02 μg/g	139, 140 [28] #14163,57, 196 [29] #141310,120
14310,615	1.51 ± 0.02	2.6 [28] #14310,119, 8.4 [29] #14310,120
15041,188	32.8 ± 0.6	
15059,240	34.9 ± 0.3	35.5 [30]
60501,105	3.6 ± 0.1 μg/g, 112 ± 2	96 [31] #60501,32
65701,23	68.3 ± 0.8	77 [32] #65700,4
72161,73	57.0 ± 0.6	58 [33] #72161,19
74220,125	300 ± 7	320, 92, 260 [34] #74220,54, #74220,54,1, #74220,54,2; 314, [31] #74220,233,19
<i>Gadolinium (μg/g)</i>		
14163,848	21 ± 7	42.7, 35.9 [35] #14163,65
60501,105	3.26 ± 0.05, 5.8 ± 0.3	
74220,125	8.1 ± 0.2, 8.6 ± 0.1	8.52 [36]
<i>Samarium (μg/g)</i>		
14163,848	24.3 ± 0.4, 29.8 ± 0.5	29.0, 36.5, 30.0 [35] #14163,65
60501,105	2.68 ± 0.04	
74220,125	6.3 ± 0.1, 6.8 ± 0.1	6.53 [36]

<sup>a</sup>For comparison, values for Geochemical Reference Sample BCR-1 were: Cd: 134 ± 1 ng/g (135 ± 1), Gd: 6.80 ± 0.05 μg/g (6.7 ± 0.8), Sm: 6.70 ± 0.05 μg/g (6.6 ± 0.8) [15]. Nominal values are shown in parentheses.

<sup>b</sup>Uncertainties are 95% confidence intervals.

there was independent evidence from isotopic measurements that sample 14163 may have been highly contaminated with terrestrial Cd. This sample displayed significant neutron capture effects in Sm and Gd but none in Cd. Also small pieces of plastic-like material were found in this sample when the sample vial was first opened.

### 3.1.2. Gadolinium and samarium

The average analytical blanks for these elements were  $74 \pm 3$  pg and  $116 \pm 9$  pg respectively. Sm can interfere with Gd at mass 152 which is the position of the  $^{152}\text{Gd}$  tracer, so Sm was always monitored at 149 or 150 during Gd concentration measurements. BaF interferences can be disregarded during Gd concentration measurements as they do not occur at isotopes 152, 158 or 160, which were used for the IDMS calculations. The Gd and Sm concentrations for sample 74220 agree with previous measurements, though for sample 14163,848 they are respectively 50% and 20% lower than the literature values. Values for Sm, and Gd concentrations in sample 60501,105 are published here for the first time.

## 3.2. Isotopic composition

Isotopic ratio measurements of Cd, Gd and Sm in five lunar samples are given in Tables 2–4, respectively.

### 3.2.1. Cadmium

The analytical blanks for the isotopic composition measurements were between 10 and 90 pg, representing less than 0.01% of the Cd in the samples. Large Cd mass fractionation reaching  $\sim 0.6\%$  per mass unit was observed in some samples (Sands et al., in preparation). A correction for this effect was made by normalizing to  $^{110}\text{Cd}/^{112}\text{Cd} = 0.51928$  using a modified version of the exponential law [19,20]. The low concentration of Cd in samples 10017,341, 14310,615, 15041,188 and 15059,240 precluded isotopic composition measurements being made because only 200-mg samples of lunar material were digested.

### 3.2.2. Gadolinium

The analytical blanks, which range from 10 pg

to 1 ng represented  $< 0.08\%$  of the Gd in the samples and had a negligible effect upon the isotopic ratios. In the presence of neutron capture, the normalizing ratio  $^{156}\text{Gd}/^{160}\text{Gd}$  will be increased by the capture of neutrons at  $^{155}\text{Gd}$ , so when samples showing neutron capture are normalized to  $^{156}\text{Gd}/^{160}\text{Gd} = 0.9361$  all the isotopes will be anomalously low. To correct for this bias the iteration method described by [21] was adopted. Normalizing ratios were determined so that  $^{156}\text{Gd}/^{160}\text{Gd} = 0.93651$ ,  $0.93654$  and  $0.93707$  for samples 14163,848 (and replicate) and 60501,105. Use of these normalizing constants increases the isotopic ratios by less than 0.0002 and 0.0004 in samples 14163 and 60501 respectively. Samples 65701,23 and 72161,73 have not been measured for Gd.

### 3.2.3. Samarium

Analytical blanks of 60 pg to 30 ng represent  $< 4\%$  of the Sm in the samples. Samples 65701,23 and 72161,73 have not been measured for Sm.

## 3.3. Neutron capture

### 3.3.1. Cadmium

The  $^{113}\text{Cd}/^{112}\text{Cd}$  and  $^{114}\text{Cd}/^{112}\text{Cd}$  ratios are plotted on a correlation diagram in Fig. 1a and are compared with the predicted path for neutron capture. Fig. 1a shows clear evidence of neutron capture on  $^{113}\text{Cd}$ . Samples 60501,105, 65701,23 and 72161,73 show changes in their  $^{114}\text{Cd}/^{113}\text{Cd}$  ratio of  $\sim 0.5\%$ . The second 60501,105 sample, shows an increase of 0.3% in  $^{114}\text{Cd}/^{113}\text{Cd}$ . The cluster of data to the lower right of Fig. 1a contains the Cd laboratory standard, BCR-1, and sample 74220,125. No neutron capture is evident in sample 74220,125 within the precision of the measurements (0.03% in the  $^{114}\text{Cd}/^{113}\text{Cd}$  ratio).

### 3.3.2. Gadolinium

The  $^{158}\text{Gd}/^{160}\text{Gd}$  versus  $^{157}\text{Gd}/^{160}\text{Gd}$  ratios are plotted on a correlation diagram in Fig. 1b and are compared with the predicted path for neutron capture. Two samples, 14163,848 and 60501,105, show evidence of neutron capture with changes of 0.4–0.8% in  $^{158}\text{Gd}/^{157}\text{Gd}$ . No neutron capture was observed for 74220,125 within experimental un-

Table 2  
Isotopic abundances<sup>a</sup> of cadmium

Sample	<sup>108</sup> Cd/ <sup>112</sup> Cd	<sup>111</sup> Cd/ <sup>112</sup> Cd	<sup>113</sup> Cd/ <sup>112</sup> Cd	<sup>114</sup> Cd/ <sup>112</sup> Cd	<sup>116</sup> Cd/ <sup>112</sup> Cd	<sup>114</sup> Cd/ <sup>113</sup> Cd
60501,105			0.50455 ± 0.00058	1.1912 ± 0.0016		2.3609 ± 0.0042
δ <sup>b</sup>			−0.31 ± 0.12	0.15 ± 0.14		0.47 ± 0.18
60501,105	0.03706 ± 0.00020	0.531499 ± 0.000096	0.50507 ± 0.00018	1.19044 ± 0.00030	0.30933 ± 0.00035	2.3570 ± 0.0010
δ			−0.21 ± 0.05	0.09 ± 0.04		0.30 ± 0.05
65701,23	0.03723 ± 0.00021	0.53070 ± 0.00025	0.50436 ± 0.00036	1.19118 ± 0.00053	0.3093 ± 0.0014	2.3618 ± 0.0020
δ			−0.35 ± 0.08	0.15 ± 0.06		0.50 ± 0.09
72161,73	0.03678 ± 0.00034	0.53067 ± 0.00032	0.50446 ± 0.00050	1.1911 ± 0.0014	0.3093 ± 0.0012	2.3610 ± 0.0036
δ			−0.33 ± 0.11	0.14 ± 0.12		0.47 ± 0.15
74220,125	0.037088 ± 0.000044	0.53092 ± 0.00017	0.506032 ± 0.000088	1.18952 ± 0.00016	0.30958 ± 0.00015	2.35068 ± 0.00051
δ			−0.02 ± 0.04	0.01 ± 0.04		0.03 ± 0.03
BCR-1	0.03709 ± 0.00011	0.531183 ± 0.000090	0.50624 ± 0.00012	1.18934 ± 0.00029	0.31046 ± 0.00015	2.34936 ± 0.00080
δ			0.02 ± 0.04	−0.00 ± 0.04		−0.03 ± 0.04
Laboratory std	0.037067 ± 0.000017	0.53111 ± 0.000012	0.50612 ± 0.00019	1.18937 ± 0.00041	0.30933 ± 0.00013	2.34997 ± 0.00042

<sup>a</sup>Cadmium isotopic ratios of samples 60501, 65701 and 72161 were corrected for Sn interference. All ratios are normalized to <sup>110</sup>Cd/<sup>112</sup>Cd = 0.51928.

<sup>b</sup>δ is the percent change in the isotopic ratio due to neutron capture. Uncertainties in this work are 95% confidence intervals for the means.

Table 3  
Isotopic abundances<sup>a</sup> of gadolinium

Sample	<sup>152</sup> Gd/ <sup>160</sup> Gd	<sup>154</sup> Gd/ <sup>160</sup> Gd	<sup>155</sup> Gd/ <sup>160</sup> Gd	<sup>156</sup> Gd/ <sup>160</sup> Gd	<sup>157</sup> Gd/ <sup>160</sup> Gd	<sup>158</sup> Gd/ <sup>160</sup> Gd	<sup>158</sup> Gd/ <sup>157</sup> Gd
14163,848	0.00970 ± 0.00081	0.10019 ± 0.00035	0.67653 ± 0.00026	0.93651 ± 0.00026	0.7147 ± 0.000612	1.13885 ± 0.00024	1.5934 ± 0.0014
δ <sup>b</sup>			−0.06 ± 0.04	0.04 ± 0.03	−0.25 ± 0.08	0.19 ± 0.02	0.43 ± 0.09
14163,848	0.00996 ± 0.00069	0.10020 ± 0.00065	0.67641 ± 0.00045	0.93654 ± 0.00045	0.71429 ± 0.00025	1.13818 ± 0.00015	1.59344 ± 0.00061
δ			−0.08 ± 0.07	0.05 ± 0.05	−0.30 ± 0.04	0.14 ± 0.01	0.44 ± 0.04
60501,105	0.0104 ± 0.0014	0.1012 ± 0.0039	0.67597 ± 0.00089	0.93707 ± 0.00089	0.71343 ± 0.00066	1.14044 ± 0.00071	1.5985 ± 0.0018
δ			−0.14 ± 0.13	0.10 ± 0.09	−0.43 ± 0.09	0.33 ± 0.06	0.76 ± 0.11
74220,125 <sup>c</sup>			0.6768 ± 0.0011	0.9361 ± 0.0011	0.71614 ± 0.00047	1.1366 ± 0.0012	1.5871 ± 0.0020
δ			−0.02 ± 0.16	0.0 ± 0.1	−0.05 ± 0.07	−0.01 ± 0.11	0.04 ± 0.13
74220,125	0.00934 ± 0.00013	0.09987 ± 0.00013	0.67673 ± 0.00013	0.9361 ± 0.0001	0.71670 ± 0.00037	1.13693 ± 0.00019	1.58634 ± 0.00087
δ			−0.03 ± 0.02	0.00 ± 0.01	0.03 ± 0.05	0.02 ± 0.02	0.01 ± 0.06
BCR-1	0.00987 ± 0.00017	0.10031 ± 0.00013	0.677030 ± 0.000038	0.9361 ± 0.0000	0.71657 ± 0.00012	1.136402 ± 0.000080	1.58589 ± 0.00033
δ			0.01 ± 0.01	0.00 ± 0.01	0.01 ± 0.02	−0.03 ± 0.01	−0.04 ± 0.02
Laboratory std	0.009355 ± 0.000062	0.099851 ± 0.000056	0.676942 ± 0.000090	0.9361	0.716471 ± 0.000094	1.136687 ± 0.000068	1.58651 ± 0.00019

<sup>a</sup>Lunar samples are normalized to a calculated <sup>156</sup>Gd/<sup>160</sup>Gd ratio (see text). Other ratios are normalized to <sup>156</sup>Gd/<sup>160</sup>Gd = 0.9361 [17].

<sup>b</sup>δ is the percent change in the isotopic ratio due to neutron capture. Uncertainties in this work are 95% confidence intervals for the means.

<sup>c</sup>Measured in peak jumping mode using Daly collector. The number of isotopes measured was minimized to maximize the precision.

Table 4  
Isotopic abundances<sup>a</sup> of samarium

Sample	<sup>144</sup> Sm/ <sup>154</sup> Sm	<sup>148</sup> Sm/ <sup>154</sup> Sm	<sup>149</sup> Sm/ <sup>154</sup> Sm	<sup>150</sup> Sm/ <sup>154</sup> Sm	<sup>152</sup> Sm/ <sup>154</sup> Sm	<sup>150</sup> Sm/ <sup>149</sup> Sm
14163,848	0.135233 ± 0.000033	0.494489 ± 0.000020	0.605559 ± 0.000023	0.325882 ± 0.000030	1.175869 ± 0.000025	0.538151 ± 0.00005 0.79 ± 0.02
δ <sup>b</sup>	0.13513 ± 0.00011	0.494375 ± 0.000064	0.6057003 ± 0.000038	0.325865 ± 0.000081	1.175712 ± 0.000047	0.53799 ± 0.00014 0.76 ± 0.03
60501,105	0.135186 ± 0.000058	0.494415 ± 0.000065	0.604644 ± 0.000054	0.326832 ± 0.000092	1.176014 ± 0.000084	0.540536 ± 0.00016 1.23 ± 0.03
δ	0.135209 ± 0.000385	0.494499 ± 0.000068	0.604795 ± 0.000080	0.32675 ± 0.000021	1.175935 ± 0.000059	0.54027 ± 0.00036 1.18 ± 0.07
74220,125	0.135209 ± 0.000029	0.494370 ± 0.000027	0.607134 ± 0.000021	0.324369 ± 0.000032	1.175768 ± 0.000036	0.534264 ± 0.000055 0.06 ± 0.02
δ	0.13531 ± 0.00005	0.49465 ± 0.00005	0.60763 ± 0.00006	0.32450 ± 0.00007	1.17619 ± 0.00007	0.53404 ± 0.00013 0.02 ± 0.02
BCR-1	0.135204 ± 0.000008	0.494292 ± 0.000057	0.607269 ± 0.000038	0.324253 ± 0.000040	1.17571 ± 0.000022	0.533953 ± 0.000074 std

<sup>a</sup>Ratios are normalized to <sup>147</sup>Sm/<sup>154</sup>Sm = 0.65914 (from [37]).

<sup>b</sup>δ is the percent change in the isotopic ratio due to neutron capture. Uncertainties in this work are 95% confidence intervals for the means.

Table 5  
Neutron fluences (ψ) for each lunar sample calculated from isotopic data in Tables 2–4<sup>a</sup>

Sample	Σ <sub>eff</sub> (10 <sup>-2</sup> cm <sup>2</sup> /g)	ψ <sup>152</sup> Gd	ψ <sup>157</sup> Gd	ψ <sup>149</sup> Sm	ψ <sup>113</sup> Cd	Literature values
14163,848	0.91	3 ± 2	2.9 ± 0.9	5.2 ± 0.2		2.81 ± 0.08 [8]
		4 ± 3	3.4 ± 0.5	4.7 ± 0.2	9 ± 3	
60501,105	0.48	< 10	3.7 ± 0.8	7.5 ± 0.2	6 ± 1	5.60 ± 0.06 [8]
				7.2 ± 0.2	10 ± 2	
65701,23	b				9 ± 3	3.7 ± 0.1 [10]
72161,73	0.85					
74220,125	0.85			0.4 ± 0.2	< 1.5	

Cross sections for each isotope are taken from Lingenfelter et al. [14]. See the text for further details. The unit of fluence is 10<sup>16</sup> neutrons/cm<sup>2</sup>.

<sup>a</sup>Uncertainties are 95% confidence intervals (this work) taking only measured uncertainties in the isotopic ratios into account.

<sup>b</sup>No value could be found in the literature for this sample. A value of 3.6 ± 0.3 × 10<sup>4</sup> cm<sup>2</sup> was used to calculate the fluence (see text).

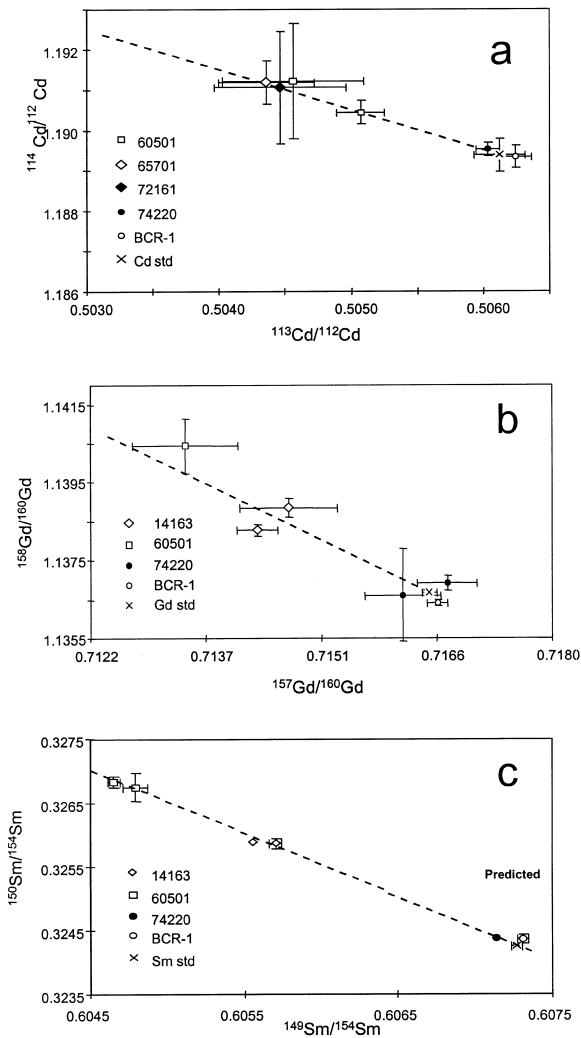


Fig. 1. Correlation diagrams showing neutron capture in lunar samples. (a)  $^{114}\text{Cd}/^{112}\text{Cd}$  versus  $^{113}\text{Cd}/^{112}\text{Cd}$ . Data are corrected for interference by Sn where necessary. (b)  $^{158}\text{Gd}/^{160}\text{Gd}$  versus  $^{157}\text{Gd}/^{160}\text{Gd}$ . (c)  $^{150}\text{Sm}/^{154}\text{Sm}$  versus  $^{149}\text{Sm}/^{154}\text{Sm}$ . Uncertainties not shown are smaller than the size of the symbol.

certainties. The changes in sample 14163,848 are the same as those found by [12], within uncertainties, and for sample 60501,105 slightly lower than those reported by [7,8].

### 3.3.3. Samarium

Fig. 1c shows  $^{150}\text{Sm}/^{154}\text{Sm}$  plotted against  $^{149}\text{Sm}/^{154}\text{Sm}$  in the three lunar samples

14163,848, 60501,105 and 74220,125 and compared to the predicted path for neutron capture. Neutron capture is seen for the first time on sample 74220,125 with an increase in  $^{150}\text{Sm}/^{149}\text{Sm}$  of 0.06%. New measurements on 14163,848 and 60501,105 show increases in  $^{150}\text{Sm}/^{149}\text{Sm}$  of 0.8 and 1.2% respectively, the same as the increase reported by [12] and [8]. The Apollo 17 sample 74220,125 is the orange glass from the rim of Shorty Crater. The small increase due to neutron capture of 0.06% is compatible with the low exposure age of 30 000 000 yr [22]. A similar change was seen by [8] in sample 74241, also from the rim of Shorty Crater, where it was probably deposited after being excavated from depth.

The neutron fluence experienced by the lunar samples was estimated using the following relationship: [23]

$$\psi = 1 \times 10^{-2} \delta_x / \sigma_x$$

where  $x$  is the isotope undergoing neutron capture,  $\delta_x$  is the percent deviation of the isotope ratio involving  $x$  from the laboratory standard and  $\sigma_x$  is its effective cross section for in  $\text{cm}^2$  as obtained from the theoretical prediction of Lingenfelter et al. [14].

Using the isotopic data from Tables 2–4 neutron fluences were calculated and are given in Table 5. Macroscopic cross sections that were used to estimate  $\sigma_x$  are shown in Table 5. These were based on literature values as discussed in the Section 3.4, except for sample 65701,23 where none was available. Because  $\sigma_x$  for  $^{113}\text{Cd}$  changes relatively slowly with macroscopic cross section ( $\Sigma_{\text{eff}}$ ) an average  $\sigma_x$  of  $3.6 \pm 0.3 \text{ cm}^2$  [14] was used in this case. Fluences obtained from our measurements fall within the range of literature values except for sample 72161,73 where it is significantly higher.

### 3.4. The neutron energy spectrum

The relative changes in the isotopic composition of, Sm, Gd and Cd in the lunar samples due to neutron capture can be used to decipher the energy spectrum of the low energy neutrons at the sites where the samples were collected. A val-



ue  $\varepsilon$  is defined as the number of neutrons captured per atom of a particular isotope [12]. It is related to experimental quantities by:

$$\varepsilon_{\text{Sm}} = \frac{[(^{150}\text{Sm}/^{149}\text{Sm})_{\text{meas}} - (^{150}\text{Sm}/^{149}\text{Sm})_{\text{terr}}]}{[1 + (^{150}\text{Sm}/^{149}\text{Sm})_{\text{meas}}]}$$

so the magnitude of  $\varepsilon_{\text{Gd}}$ ,  $\varepsilon_{\text{Sm}}$  and  $\varepsilon_{\text{Cd}}$  for the relevant neutron capture cross section, will reflect the intensity of the thermal neutrons at each energy. The calculated values of,  $\varepsilon_{\text{Gd}}$ ,  $\varepsilon_{\text{Sm}}$  and  $\varepsilon_{\text{Cd}}$  are listed in Table 6. The changes in Gd and Sm,  $\varepsilon_{^{157}\text{Gd}}$  and  $\varepsilon_{\text{Sm}}$ , for sample 14163,848 are the same as found by [12]. For sample 60501,105, our  $\varepsilon_{^{157}\text{Gd}}$  is 30% lower, and  $\varepsilon_{\text{Sm}}$  is the same as, the values reported in [8]. In sample 72161,73 only Cd was measured, so  $\varepsilon_{^{157}\text{Gd}}$  and  $\varepsilon_{\text{Sm}}$  from [10] are included in Table 6 for comparison purposes.

Studies described in [6–10,24] compared measurements of the ratio  $\varepsilon_{\text{Sm}}/\varepsilon_{\text{Gd}}$  with the expected theoretical values [14] and obtained higher values, which indicated a harder neutron energy spectrum than expected in the lunar soil. The additional measurements of Cd presented in this paper allow a significant extension of these comparisons to a higher energy by plotting  $\varepsilon_{\text{Cd}}/\varepsilon_{\text{Gd}}$  and  $\varepsilon_{\text{Cd}}/\varepsilon_{\text{Sm}}$ .

The ratios  $\varepsilon_{\text{Cd}}/\varepsilon_{\text{Gd}}$ ,  $\varepsilon_{\text{Cd}}/\varepsilon_{\text{Sm}}$  and  $\varepsilon_{\text{Sm}}/\varepsilon_{\text{Gd}}$  from this work and the literature are listed in Table 6 and plotted against  $\Sigma_{\text{eff}}$ , the macroscopic cross section, in Fig. 1a–c. The ratios  $\varepsilon_{\text{Cd}}/\varepsilon_{\text{Gd}}$ ,  $\varepsilon_{\text{Cd}}/\varepsilon_{\text{Sm}}$  and  $\varepsilon_{\text{Sm}}/\varepsilon_{\text{Gd}}$  are a measure of the neutron energy spectrum below 0.2 eV and are compared here to the theoretical values determined by Lingenfelter et al. [14].  $\varepsilon_{\text{Cd}}/\varepsilon_{\text{Gd}}$ ,  $\varepsilon_{\text{Cd}}/\varepsilon_{\text{Sm}}$  and  $\varepsilon_{\text{Sm}}/\varepsilon_{\text{Gd}}$  for sample

72161,73 are calculated with  $\varepsilon_{\text{Cd}}$  from this work and  $\varepsilon_{\text{Gd}}$  and  $\varepsilon_{\text{Sm}}$  from [10].

The macroscopic cross section ( $\Sigma_{\text{eff}}$ ) is calculated from the neutron capture cross section of the individual elements that make up the soil where the sample was found [14]. Published values needed to estimate neutron fluences are shown in Table 5. These were taken from reference [8] for sample 60501, 105. The value for the Apollo 14 basalt, 14163,848 was taken to be the same as given for 14148 [8], a surface sample with similar composition to 14163,848. Also for sample 74220,125 the value given by [8] for sample 74241 was used (see Section 3.3). The value used for sample 72161,73 was taken from [10]. Included in  $\Sigma_{\text{eff}}$  are Si, Ti, Al, Fe, Mg, Ca, Gd, Sm, Eu, O, Mn, Cr, Na and K, all elements which have significant neutron capture cross sections at thermal energies. No value could be found for sample 65701,23.

The measured  $\varepsilon_{\text{Sm}}/\varepsilon_{\text{Gd}}$  values are plotted against  $\Sigma_{\text{eff}}$  in Fig. 2a. Sample 14163,848 has the same  $\varepsilon_{\text{Sm}}/\varepsilon_{\text{Gd}}$  value as [6] within experimental uncertainties ( $1.0 \pm 0.3$  and  $1.0 \pm 0.1$  in this work, compared with  $0.89 \pm 0.03$  in [6]). In sample 60501,105 our value of  $0.9 \pm 0.2$  for  $\varepsilon_{\text{Sm}}/\varepsilon_{\text{Gd}}$  is greater than that found by [8] ( $0.61 \pm 0.02$ ). Other published  $\varepsilon_{\text{Sm}}/\varepsilon_{\text{Gd}}$  data, [12,25], are 15–20% above the theoretical curve, although the uncertainties on this curve are  $\pm 30\%$ . Our data are therefore generally consistent with earlier data for these elements which confirms there was a harder neutron energy spectrum than predicted by [14].

New data are presented here for Cd. The

Table 6

$\varepsilon_{^{155}\text{Gd}}$ ,  $\varepsilon_{^{157}\text{Gd}}$ ,  $\varepsilon_{\text{Sm}}$  and  $\varepsilon_{\text{Cd}}$ , the number of neutrons captured per atom of a particular isotope, and ratios of these quantities, for the lunar samples measured in this work<sup>a</sup>

Sample	$\varepsilon_{^{155}\text{Gd}}$ ( $10^{-3}$ )	$\varepsilon_{^{157}\text{Gd}}$ ( $10^{-3}$ )	$\varepsilon_{\text{Sm}}$ ( $10^{-3}$ )	$\varepsilon_{\text{Cd}}$ ( $10^{-3}$ )	$\varepsilon_{\text{Cd}}/\varepsilon_{\text{Gd}}$	$\varepsilon_{\text{Cd}}/\varepsilon_{\text{Sm}}$	$\varepsilon_{\text{Sm}}/\varepsilon_{\text{Gd}}$	Literature values $\varepsilon_{\text{Sm}}/\varepsilon_{\text{Gd}}$
14163,848	$0.6 \pm 0.3$	$2.7 \pm 0.6$	$2.73 \pm 0.06$				$1.0 \pm 0.2$	$0.89 \pm 0.03$ [12]
	$0.7 \pm 0.5$	$2.7 \pm 0.2$	$2.6 \pm 0.1$				$1.0 \pm 0.1$	
60501,105			$4.3 \pm 0.1$	$3.3 \pm 1.3$		$0.8 \pm 0.4$		
	$1.4 \pm 0.7$	$4.6 \pm 0.7$	$4.1 \pm 0.2$	$2.1 \pm 0.3$	$0.5 \pm 0.2$	$0.5 \pm 0.2$	$0.9 \pm 0.2$	$0.61 \pm 0.02$ [8]
65701,23				$3.5 \pm 0.6$				
72161,73		$(4.2) (\pm 0.1)$	$(3.1) (\pm 0.1)$	$3.3 \pm 1.1$	$(0.8) (\pm 0.3)$	$(1.1) (\pm 0.3)$		$0.75 \pm 0.06$ [10]
74220,125		$-0.1 \pm 0.4$	$0.20 \pm 0.06$	$0.2 \pm 0.2$				

The brackets indicate those values of  $\varepsilon_{\text{Gd}}$  and  $\varepsilon_{\text{Sm}}$  for sample 72161 taken from [10].

<sup>a</sup>Uncertainties are 95% confidence intervals (this work) and two standard deviations of the mean [8,10,12].

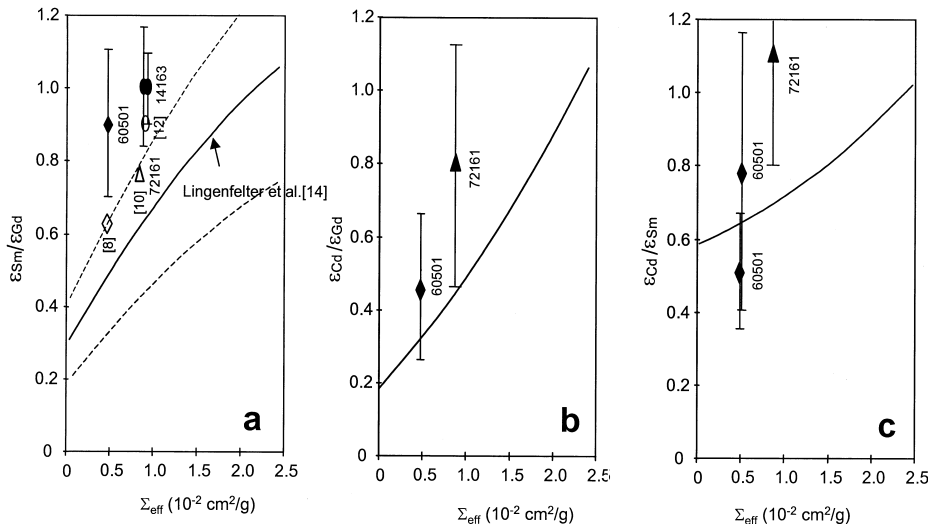


Fig. 2. The neutron energy spectrum in lunar samples. Data are compared with the theoretical model of Lingenfelter [14]. Data from this work are shown as filled symbols, while previous measurements are shown as open symbols. Labels in parentheses identify previously published data. (a)  $\epsilon_{\text{Sm}}/\epsilon_{\text{Gd}}$  versus  $\Sigma_{\text{eff}}$ . (b)  $\epsilon_{\text{Cd}}/\epsilon_{\text{Gd}}$  versus  $\Sigma_{\text{eff}}$ .  $\epsilon_{\text{Gd}}$  used for 72161,73 which is from [10]. (c)  $\epsilon_{\text{Cd}}/\epsilon_{\text{Sm}}$  versus  $\Sigma_{\text{eff}}$ .  $\epsilon_{\text{Sm}}$  used for 72161,73 which is from [10].

$\epsilon_{\text{Cd}}/\epsilon_{\text{Sm}}$ ,  $\epsilon_{\text{Cd}}/\epsilon_{\text{Gd}}$  ratios shown in Fig. 2b,c are generally higher than predicted although one  $\epsilon_{\text{Cd}}/\epsilon_{\text{Sm}}$  value for sample 60501,105 is lower. The precision of the measurements on sample 72161,73 place it significantly above the theoretical curve at the 95% confidence level, assuming no uncertainty on the theoretical values. The Cd data therefore also lend support for a harder neutron energy spectrum that was used by Lingenfelter et al. [14].

These results are consistent with the outcome of the Lunar Neutron Probe Experiment [26] which showed that Lingenfelter et al. [14] calculated too many low energy neutrons.

#### 4. Conclusions

The concentrations of Cd, Gd and Sm in nine lunar samples have also been measured by IDMS with Cd being measured for the first time by this method. The measured Gd and Sm concentrations include values for sample 14163,848 which are significantly lower than the literature values.

Neutron capture effects in Cd, Gd and Sm have been measured in five lunar samples. Changes in

the Cd isotopic ratios, reported for the first time in lunar material, reach  $\sim 0.5\%$  for  $^{114}\text{Cd}/^{113}\text{Cd}$  in samples 60501,105, 65701,23 and 72161,73. For Gd, the  $^{158}\text{Gd}/^{157}\text{Gd}$  ratio shows increases of 0.4% and 0.8% in samples 14163,848 and 60501,105 respectively, confirming earlier measurements of the former, but significantly lower for the latter sample. The  $^{150}\text{Sm}/^{149}\text{Sm}$  ratio shows increases of 0.8%, 1.2% and 0.06% in samples 14163,848, 60501,105 and 74220,125, respectively, which confirm and extend earlier measurements.

A comparison of the changes caused by thermal neutron capture on Gd, Sm and Cd isotopic ratios have allowed an examination of the relative intensity of neutrons with energies of 0.03 eV, 0.09 eV and 0.178 eV, respectively. Neutron fluences are consistent with previous work except for sample 72161,73 where the literature value is significantly lower. Results for Gd and Sm support earlier work that concluded the neutron energy spectrum was harder than expected from theoretical models of Lingenfelter et al. [14]. These conclusions are further supported in this study by Cd data that reach statistical significance for sample 72161,73.

## Acknowledgements

The authors acknowledge the provision of nine lunar samples by NASA to J.R. De Laeter, the designated Principal Investigator for these studies, and the assistance of the NASA lunar sample curators. During this project helpful technical support and advice was received from staff and colleagues, in particular R. Loss, W. Chisholm, G. Burton, D. Nelson, I. Fletcher, C. Smith, R. Maas, and T. Margrain. The Curtin TIMS laboratory is supported by funds from the Australian Research Council. One of us (D.G.S.) was supported during this work by a Curtin University Postgraduate Research Scholarship, an Isotope Studies Scholarship and an A.F.U.W.(WA) Inc Mary Walters Memorial bursary. *[FA]*

## References

- [1] O. Eugster, F. Tera, D.S. Burnett, G.J. Wasserburg, Neutron capture effects in Gd from the Norton County meteorite, *Earth Planet. Sci. Lett.* 7 (1970) 436–440.
- [2] H. Hidaka, M. Ebihara, S. Yoneda, Sm and Gd isotopic compositions of meteorites, *Meteorit. Planet. Sci.* 32 (1997) 59.
- [3] O. Eugster, F. Tera, D.S. Burnett, G.J. Wasserburg, The isotopic composition of Gd and the neutron capture effects in samples from Apollo 11, *Earth Planet. Sci. Lett.* 8 (1970) 20–30.
- [4] G.W. Lugmair, K. Marti, Neutron capture effects in lunar Gd and the irradiation histories of some lunar rocks, *Earth Planet. Sci. Lett.* 13 (1971) 32–42.
- [5] D.S. Burnett, J.C. Huneke, F.A. Podosek, G.P. Russ, G.J. Wasserburg, The irradiation history of lunar samples. *Proc. Lunar Sci. Conf. 2nd, Geochim. Cosmochim. Acta* 2 (Suppl.) (1971) 1671–1679.
- [6] G.P. Russ, D.S. Burnett, G.J. Wasserburg, Lunar neutron stratigraphy, *Earth Planet. Sci. Lett.* 15 (1972) 172–186.
- [7] G.P. Russ, Apollo 16 neutron stratigraphy, *Earth Planet. Sci. Lett.* 17 (1973) 275–289.
- [8] D.B. Curtis, G.J. Wasserburg, Apollo 17 neutron stratigraphy-sedimentation and mixing in the lunar regolith, *The Moon* 13 (1975) 185–227.
- [9] D.B. Curtis, G.J. Wasserburg, Stratigraphic processes in the lunar regolith – additional insight from neutron fluence measurements on bulk soils and lithic fragments from the deep drill cores. *Proc. Lunar Sci. Conf. 8th* (1977) 3575–3593.
- [10] D.B. Curtis, G.J. Wasserburg, Transport and erosional processes in the Taurus–Littrow Valley – inferences from neutron fluences in surface soils. *Proc. Lunar Sci. Conf. 8th* (1977) 3045–3057.
- [11] D.D. Bogard, L.E. Nyquist, B.M. Bansal, D.H. Garrison, H. Wiesmann, G.F. Herzog, A.A. Albrecht, S. Vogt, J. Klein, Neutron-capture  $^{36}\text{Cl}$ ,  $^{41}\text{Ca}$ ,  $^{36}\text{Ar}$ , and  $^{150}\text{Sm}$  in large chondrites: Evidence for high fluences of thermalized neutrons, *J. Geophys. Res.* 100 (1995) 9401–9416.
- [12] G.P. Russ, D.S. Burnett, R.E. Lingenfelter, G.J. Wasserburg, Neutron capture on  $^{149}\text{Sm}$  in lunar samples, *Earth Planet. Sci. Lett.* 13 (1971) 53–63.
- [13] K.J.R. Rosman, J.R. De Laeter, A survey of cadmium isotopic abundances, *J. Geophys. Res.* 83 (1978) 1279–1287.
- [14] R.E. Lingenfelter, E.H. Canfield, V.E. Hampel, The lunar neutron flux revisited, *Earth Planet. Sci. Lett.* 16 (1972) 355–369.
- [15] D.G. Sands, K.J.R. Rosman, Cd, Gd and Sm concentrations in BCR-1, BHVO-1, BIR-1, DNC-1, MAG-1, PCC-1 and W-2 by isotope dilution thermal ionisation mass spectrometry, *J. Geostand. Geanal.* 21 (1997) 77–83.
- [16] I.W. Croudace, S. Marshall, Determination of rare earth elements and yttrium in nine geochemical reference samples using a novel group separation procedure involving mixed-acid elution ion-exchange chromatography, *Geostand. Newslett.* 15 (1991) 139–144.
- [17] O. Eugster, F. Tera, D.S. Burnett, G.J. Wasserburg, Isotopic composition of Gd and neutron-capture effects in some meteorites, *J. Geophys. Res.* 75 (1970) 2753–2768.
- [18] K.G. Heuman, Isotope dilution mass spectrometry (IDMS) of the elements, *Mass Spectrom. Rev.* 11 (1992) 41–67.
- [19] D.G. Sands, Lunar neutron energy spectra from isotope abundance measurements on Cd, Sm and Gd. Ph.D. Thesis, Curtin University of Technology, Perth, W.A., 1999, p. 244.
- [20] W.A. Russell, D.A. Papanastassiou, T.A. Tombrello, Ca isotope fractionation on the Earth and other solar system materials, *Geochim. Cosmochim. Acta* 42 (1978) 1075–1090.
- [21] H. Hidaka, M. Ebihara, M. Shima, Determination of the isotopic compositions of Sm and Gd by thermal ionization mass spectrometry, *Anal. Chem.* 67 (1995) 1437–1441.
- [22] R. Arvidson, G. Crozaz, R.J. Drozd, C.M. Hohenberg, C.J. Morgan, Cosmic ray exposure ages of features and events at the Apollo landing sites, *The Moon* 13 (1975) 259–276.
- [23] H. Hidaka, M. Ebihara, S. Yoneda, Neutron capture effects on samarium, europium, and gadolinium in Apollo 15 deep drill core samples, *Meteorit. Planet. Sci.* 35 (2000) 581–589.
- [24] G.P. Russ, Neutron capture on Gd and Sm in the Luna 16, G-2 Soil, *Earth Planet. Sci. Lett.* 13 (1972) 384–386.
- [25] D.S. Burnett, D.S. Woolum, Lunar neutron capture as a tracer for regolith dynamics. *Proc. Lunar Sci. Conf. 5th, Geochim. Cosmochim. Acta* 2 (Suppl.) (1974) 2061–2074.

- [26] D.S. Woolum, D.S. Burnett, M. Furst, J.R. Weiss, Measurements of the lunar neutron density profile, *The Moon* 12 (1975) 231–250.
- [27] E. Anders, R. Ganapathy, R. Keays, J.C. Laul, J.W. Morgan, Volatile and siderophile elements in lunar rocks Comparison with terrestrial and meteoritic basalts. *Proc. Lunar Sci. Conf. 2nd*, *Geochim. Cosmochim. Acta* 2 (Suppl.) (1971) 1021–1036.
- [28] J.W. Morgan, J.C. Laul, U. Krahenbuhl, R. Ganapathy, E. Anders, Major impacts on the moon: Characterization from trace elements in Apollo 12 and 14 samples. *Proc. Lunar Sci. Conf. 3rd*, *Geochim. Cosmochim. Acta* 2 (Suppl.) (1972) 1377–1395.
- [29] P.A. Baedeker, C.-L. Chou, J.T. Wasson, The extra lunar component in lunar soils and breccias. *Proc. Lunar Sci. Conf. 3rd*, *Geochim. Cosmochim. Acta* 2 (Suppl.) (1972) 1343–1359.
- [30] G. Ryder (Ed.), *Catalog of Apollo 15 Rocks, Part 1*, NASA, Lyndon B. Johnson Space Center, Houston, TX, 1985, pp. 15015–15299.
- [31] J.T. Wasson, C.-L. Chou, K.L. Robinson, P.A. Baedeker, Siderophiles and volatiles in Apollo 16 rocks and soils, *Geochim. Cosmochim. Acta* 39 (1975) 1475–1485.
- [32] W.V. Boynton, C.-L. Chou, K.L. Robinson, P.H. Warren, J.T. Wasson, Lithophiles, siderophiles and volatiles in Apollo 16 soils and rocks. *Proc. Lunar Sci. Conf. 7th*, *Geochim. Cosmochim. Acta* 1 (Suppl.) (1976) 727–742.
- [33] P.A. Baedeker, C.-L. Chou, L.L. Sundberg, J.T. Wasson, Volatile and siderophilic trace elements in the soils and rocks of Taurus–Littrow. *Proc. Lunar Sci. Conf. 5th*, *Geochim. Cosmochim. Acta* 2 (Suppl.) (1974) 1625–1643.
- [34] J.W. Morgan, R. Ganapathy, H. Higuchi, U. Krahenbuhl, E. Anders, Lunar basins: Tentative characterization of projectiles, from meteoritic elements in Apollo 17 boulders. *Proc. Lunar Sci. Conf. 5th*, *Geochim. Cosmochim. Acta* 2 (Suppl.) (1974) 1703–1736.
- [35] N.J. Hubbard, P.W. Gast, J.M. Rhodes, B.M. Bansal, S.E. Wiesmann, H. Church, Nonmare basalts Part II. *Proc. Lunar Sci. Conf. 3rd*, *Geochim. Cosmochim. Acta* 2 (Suppl.) (1972) 1161–1179.
- [36] B.V.S.P., *Basaltic Volcanism in the Terrestrial Planets*, Pergamon, New York, 1981.
- [37] G.W. Lugmair, N.B. Scheinin, K. Marti, Sm–Nd Age and History of Apollo 17 Basalt 75075: Evidence for Early Differentiation of the Lunar Exterior. *Proc. Lunar Sci. Conf. 6th* (1975) 1419–1429.